

# Glueballs on a transverse lattice

S. Dalley\* and B. van de Sande\*\*

*\*Department of Applied Mathematics and Theoretical Physics,  
Silver Street, Cambridge CB3 9EW, England*

*\*\*Geneva College,  
3200 College Ave., Beaver Falls, PA 15010*

## Abstract

Accurate non-perturbative calculations of glueballs are performed using light-front quantised  $SU(N)$  gauge theory, to leading order of the  $1/N$  expansion. Based on early work of Bardeen and Pearson, disordered gauge-covariant link variables  $M$  on a coarse transverse lattice are used to approximate the physical gauge degrees of freedom. Simple energetics imply that, at lattice spacings of order the inverse QCD scale, the effective light-front Hamiltonian can be expanded in gauge-invariant powers of  $M$ : a colour-dielectric expansion. This leads to a self-consistent constituent structure of boundstates. We fix the couplings of this expansion by optimising Lorentz covariance of low-energy eigenfunctions. To lowest non-trivial order of the expansion, we have found a one-parameter trajectory of couplings that enhances Lorentz covariance. On this trajectory the masses of nearly-covariant glueball states exhibit approximate scaling, having values consistent with large- $N$  extrapolations of continuum results from other methods. There is very little variation with  $N$  in pure Yang-Mills theory: the lightest glueball mass changes by only a few percent between  $SU(3)$  and  $SU(\infty)$ . The corresponding light-front wavefunctions show an unconventional structure. We also examine restoration of rotational invariance in the heavy-source potential.

# 1 Introduction

There are few, if any, efficient methods for tackling relativistic strongly-bound states in generic four-dimensional gauge theories. The canonical example is QCD, where non-perturbative theoretical calculations have rarely been ahead of experiment. Future progress in particle physics is likely to hinge upon a detailed theoretical understanding of these questions. This has led some theorists to develop Hamiltonian quantisation on a light-front [1, 2]. In the presence of suitable high-energy cut-offs, the light-front vacuum state is trivial and wavefunctions built upon it are Lorentz boost-invariant.

In particular, Brodsky and Lepage [3] and Pauli and Brodsky [4] have urged the development of the light-front quantisation of QCD (LFQCD). More recently, Wilson *et al.* [5] have clarified the physical principles underlying LFQCD and suggested a weak-coupling calculational framework. In this paper we develop an alternative framework which appears promising: a light-front quantisation of lattice gauge theory [6]. Calculations that we have already performed with this method [8, 9, 10], for non-Abelian gauge theories in  $2 + 1$  dimensions, were surprisingly successful in comparison to results from traditional Euclidean lattice path integral simulations (ELMC) [11]. They have also produced new results in the form of the light-front wavefunctions, the starting point for investigation of virtually any physically interesting observable. Encouraged by this success, we investigate here the glueballs and heavy-source potential in  $3 + 1$ -dimensional gauge theory without fermions.

The well-known triviality of the light-front vacuum may be reconciled with the conventional picture of a complicated QCD vacuum. In light-front co-ordinates, vacuum structure is carried by an isolated set of (infinitely) high energy modes, which are removed by the cut-off. According to standard lore, one would expect that appropriate renormalisation of the Hamiltonian and other observables would recover the information excised by the high-energy cut-off. In this way, effects normally associated with the vacuum, such as spontaneous symmetry breaking, must appear explicitly in the Hamiltonian. But the non-perturbative renormalisation group (RG) formalism to systematically compute the necessary counter-terms does not yet exist. Efforts are being made to formulate a perturbative light-front RG for QCD [12], but the full vacuum structure must necessarily appear via counter-terms that are non-analytic in the perturbative couplings. Faced with the problem of finding non-perturbatively renormalised Hamiltonians, we will use symmetry as our guide.

The first step is to choose the most general set of Hamiltonians which respect symmetries of the theory that are not violated by the cut-offs. After truncating this set according to some reasonable criteria, we non-perturbatively test the low-energy eigenfunctions and eigenvalues for restoration of the symmetries violated by the cut-offs. These tests, rather than RG transformations, are used to explore the space of Hamiltonians. Since we maintain gauge invariance, the symmetries in question involve only Lorentz covariance. We will remove all but one cut-off and find that our truncated space of Hamiltonians contains a unique one-parameter trajectory  $\mathcal{T}_s$  on which Lorentz covariance is greatly enhanced. The validity of  $\mathcal{T}_s$  is confirmed by the approximate scaling of low-energy physical quantities along this trajectory.  $\mathcal{T}_s$  will be used as the basis for extracting cut-off independent results. This is a first-principles approach, since no data are taken from experiment (aside from the overall scale in QCD).

Apart from Lorentz invariance, we must address the issue of gauge invariance. One knows that gauge invariance can be maintained with lattice cut-offs and compact variables [13, 14]. However, in

light-front coordinates a high-energy lattice cut-off can only be applied to the transverse directions; the null direction on the initial surface must remain continuous. Also, if one were to employ the usual formulation of lattice gauge theory with degrees of freedom in  $SU(N)$ , it is not straightforward to identify the independent degrees of freedom that are essential for canonical Hamiltonian quantisation. The tricks of ‘equal-time’ Hamiltonian lattice gauge theory in temporal gauge [14] do not carry over to light-front Hamiltonian lattice gauge theory in any convenient way [15]. One does not have to choose lattice variables in  $SU(N)$  however. It was noted long ago by Bardeen and Pearson [6], that lattice variables  $M$  in the space of all complex  $N \times N$  matrices were physically more appropriate on a coarse lattice. Gauge invariance is maintained and it is straightforward to identify the independent degrees of freedom. The penalty is that one is too far from the continuum to use weak-coupling perturbation theory. But in the case of light-front Hamiltonians, this may be of limited use anyway. Bardeen *et al.* [7] suggested that on coarse lattices one could expand the light-front Hamiltonian in powers of  $M$  (a kind of strong-coupling expansion). The validity of this expansion is subtle however, since it rests on the dynamical properties of light-front Fock states in this kind of theory, in particular the weakness of couplings between sectors with different number of partons [16].

Expanding the light-front Hamiltonian of  $SU(N)$  gauge theory to leading non-trivial order in  $M$  and  $1/N$ , we find the trajectory of couplings  $\mathcal{T}_s$  mentioned above. In the region of coupling space we are able to investigate, the transverse lattice spacing on  $\mathcal{T}_s$  is found to be always greater than about 0.65 fm. However, Lorentz covariance and scaling are present to sufficient accuracy that we can make direct estimates of the continuum values of low-energy observables.<sup>1</sup>

The organisation of the paper is as follows. In the first part of the present work, we give a systematic treatment of transverse lattice gauge theory. In Section 2 we construct generic light-front Hamiltonians on the transverse lattice and introduce approximation schemes for studying them; in particular, we review the ‘colour-dielectric’ expansion in powers of  $M$  that leads to a constituent picture of boundstates. By working to leading order in  $1/N$ , the transverse dynamics dimensionally reduce (for a coarse lattice) [10], the problem becoming mathematically equivalent to a 1 + 1-dimensional gauge theory with adjoint matter [16]. As well as the lattice cut-off, which can only be used in transverse spatial directions, we also employ null-plane boundary conditions, specifically Discrete Light-Cone Quantisation (DLCQ) [4], and Tamm-Dancoff cut-offs for transverse degrees of freedom. The latter gauge-invariant cut-offs can be removed by extrapolation to give finite answers for fixed transverse lattice spacing, the only remaining cut-off.

The renormalisation of the theory at fixed lattice spacing is then accomplished by optimising Lorentz covariance, discussed in Section 3. This amounts to a choice of ‘metric’ in the space of Hamiltonians, based on explicit calculations of observables. Results from our calculations are presented in Section 4; we will not describe in any detail the calculational techniques, but refer the reader to our previous papers. Some preliminary results from the glueball calculations were presented in Ref. [17], but the new material here is more accurate and extensive, including a thorough analysis of the space of couplings, the glueball masses and wavefunctions, and the heavy-source system.

We end this introduction by quoting the most readily understandable of our main results: the lowest glueball masses. We estimate the lightest glueball in  $SU(\infty)$  gauge theory, the  $\mathcal{J}^{PC} = O^{++}$ , to be at a mass  $M_{O^{++}} = 3.50 \pm 0.24\sqrt{\sigma}$ , where  $\sigma$  is the string tension. This is essentially

---

<sup>1</sup>As with other ‘strong-coupling’ approaches, the question of the formal connection to the continuum limit is not directly answered.

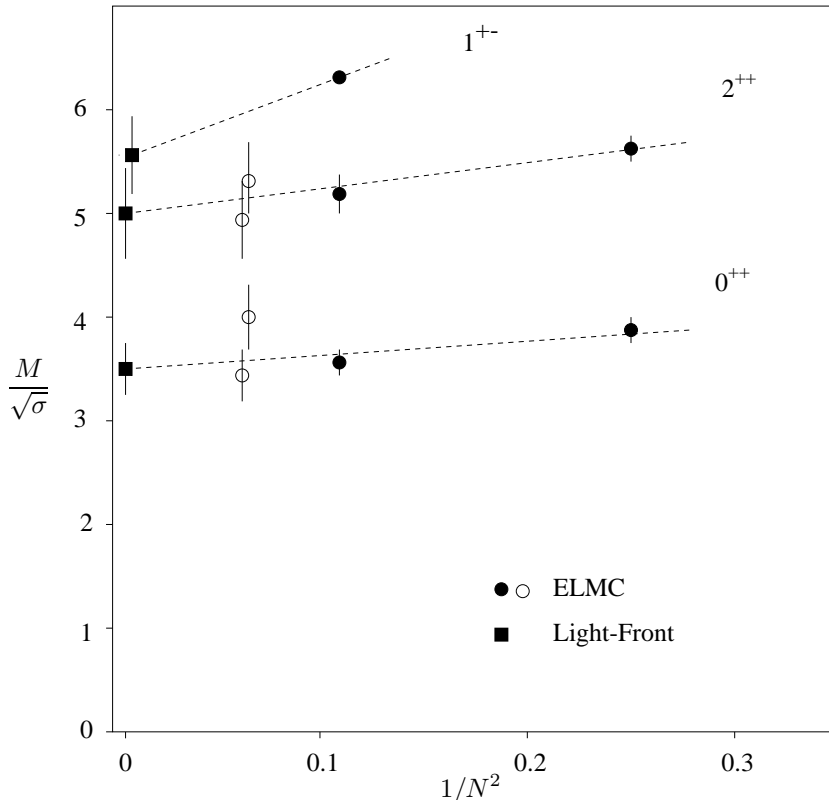


Figure 1: The variation of glueball masses with  $N$  (pure glue). ELMC predictions are continuum ones for  $N = 2, 3$  [19, 18, 20] and fixed lattice spacing estimates for  $N = 4$  [35]. The dotted lines are to guide the eye and correspond to leading linear dependence on  $1/N^2$ .

indistinguishable from the result for  $SU(3)$  pure gauge theory established rigorously by ELMC in recent years [18]. For the  $2^{++}$  tensor state, not all components of the multiplet are yet behaving covariantly; but from those components which are reliable, we estimate  $M_{2^{++}} = 4.97 \pm 0.43\sqrt{\sigma}$ . The vector  $1^{+-}$  has  $M_{1^{+-}} = 5.57 \pm 0.4\sqrt{\sigma}$ . We find no light pseudo-scalar  $0^{-+}$ , but suspect our candidate for this has a large error. These results are summarised in Figure 1. Other recent estimates of glueball masses have been obtained in  $SU(3)$  Hamiltonian gauge theory [21] and based on extensions of the Maldacena conjecture for large- $N$  gauge theory [22], though we consider those results to be less rigorous than ours.

## 2 Transverse lattice Hamiltonians.

### 2.1 Energy-momentum

In 3+1 spacetime dimensions we introduce a square lattice of spacing  $a$  in the ‘transverse’ directions  $\mathbf{x} = \{x^1, x^2\}$  and a continuum in the  $\{x^0, x^3\}$  directions. In light-front (LF) co-ordinates  $x^\pm = (x^0 \pm x^3)/\sqrt{2}$ , we treat  $x^+$  as canonical time and place anti-periodic boundary conditions on  $x^- \sim x^- + \mathcal{L}$ . Both  $1/a$  and  $\mathcal{L}$  are high-energy cut-offs for the LF Hamiltonian  $P^- = (P^0 - P^3)/\sqrt{2}$  that evolves the system in LF time  $x^+$ . The Lorentz indices  $\mu, \nu \in \{0, 1, 2, 3\}$  are split into LF indices  $\alpha, \beta \in \{+, -\}$

and transverse indices  $r, s \in \{1, 2\}$ .

The gauge field degrees of freedom below the cut-offs are represented by Hermitian gauge potentials  $A_\alpha(\mathbf{x})$  and complex link variables  $M_r(\mathbf{x})$ . We also introduce heavy scalar sources  $\phi(\mathbf{x})$ . On the transverse lattice,  $A_\alpha(\mathbf{x})$  and  $\phi(\mathbf{x})$  are associated with a site  $\mathbf{x}$ , while  $M_r(\mathbf{x})$  is associated with the link from  $\mathbf{x}$  to  $\mathbf{x} + a\hat{r}$ . Each ‘site’  $\mathbf{x}$  is in fact a two-dimensional plane spanned by  $\{x^+, x^-\}$ . These variables transform under transverse lattice gauge transformations  $U \in SU(N)$  as

$$\begin{aligned} A_\alpha(\mathbf{x}) &\rightarrow U(\mathbf{x})A_\alpha(\mathbf{x})U^\dagger(\mathbf{x}) + i(\partial_\alpha U(\mathbf{x}))U^\dagger(\mathbf{x}) \\ M_r(\mathbf{x}) &\rightarrow U(\mathbf{x})M_r(\mathbf{x})U^\dagger(\mathbf{x} + a\hat{r}) \end{aligned} \quad (1)$$

$$\phi(\mathbf{x}) \rightarrow U(\mathbf{x})\phi(\mathbf{x}). \quad (2)$$

Since it will be possible to eliminate  $A_\alpha$  by partial gauge-fixing,  $M$  and  $\phi$  represent the physical transverse polarisations. The simplest gauge covariant combinations are  $M$ ,  $\phi$ ,  $F^{\alpha\beta}$ ,  $\det M$ ,  $\overline{D}^\alpha M$ ,  $D^\alpha \phi$ , where the covariant derivatives are

$$\overline{D}_\alpha M_r(\mathbf{x}) = (\partial_\alpha + iA_\alpha(\mathbf{x})) M_r(\mathbf{x}) - iM_r(\mathbf{x})A_\alpha(\mathbf{x} + a\hat{r}) \quad (3)$$

$$D_\alpha \phi = \partial_\alpha \phi + iA_\alpha \phi. \quad (4)$$

From these we wish to construct general LF Hamiltonians  $P^-$  invariant under gauge transformations and those Lorentz transformations unviolated by the cut-offs.

To proceed, we must make some assumptions about which finite sets of operators to include in the calculation. Since symmetries will be tested explicitly, a poor choice of operators would show up later on. The following criteria were used to select operators in  $P^-$  for pure gauge theory:

- (A) Canonical quadratic form for  $P^+$ ;
- (B) Naïve parity restoration as  $\mathcal{L} \rightarrow \infty$ ;
- (C) Transverse locality;
- (D) Expansion in gauge-invariant powers of  $M$ .

Each of these criteria deserves some explanation. The last three can all be straightforwardly checked in principle by systematically relaxing the condition.

- (A) Of the generators of the Poincaré group  $\{P^+, P^-, P^r, M^{\mu\nu}\}$ , the subset  $\{P^r, P^+, M^{+r}, M^{12}, M^{+-}\}$  can usually be made kinematic. That is, they can be made independent of interactions, quadratic in the fields. The imposition of a lattice cut-off can spoil this property, especially if one wants to maintain gauge invariance. We try to maintain as many operators as possible in kinematic form, consistent with gauge invariance. Further details are given below, but for now we note that condition (A) can be satisfied in light-front gauge  $A_- = 0$  by using a Lagrangian containing the only  $x^+$ -dependent gauge-covariant term quadratic in link fields,  $\overline{D}_\alpha M_r(\mathbf{x})(\overline{D}^\alpha M_r(\mathbf{x}))^\dagger$ . Although higher order terms in  $M$  cannot be ruled out, only with a quadratic term is quantisation straightforward and, even then, only in the LF gauge  $A_- = 0$ .
- (B) We will extrapolate to the  $\mathcal{L} \rightarrow \infty$  limit in the longitudinal direction, deriving  $P^-$  from a Lagrangian including only dimension 2 operators with respect to  $\{x^+, x^-\}$  co-ordinates. It has

been noted that functions of dimensionless ratios of longitudinal momenta  $p^+$  can appear in couplings of boost-invariant LF Hamiltonians [5]. However, these functions must be strongly constrained by LF parity  $x^+ \leftrightarrow x^-$ . Parity is a dynamical symmetry on the light-front (it does not preserve the quantisation surface) and is difficult to check explicitly. We will assume<sup>2</sup> that, if  $P^-$  is derived from a Lagrangian with naïve  $x^+ \leftrightarrow x^-$  symmetry ( $p^+$ -independent couplings), then parity is correctly restored in transverse lattice gauge theory in the limit  $\mathcal{L} \rightarrow \infty$ . Although DLCQ treatments of analogous 1 + 1-dimensional gauge theories have been successful under similar assumptions [16, 24, 25], in the present case there are many more possible operators that are ruled out by conditions (A) and (B) combined.

- (C) In products of gauge-invariant operators on the transverse lattice, each term of the product can be arbitrarily separated in the transverse direction. We assume some transverse locality by restricting products of gauge invariant operators to share at least one site  $\mathbf{x}$ .
- (D) After fixing to LF gauge  $A_- = 0$  and eliminating the resultant constrained field  $A_+$ , Fock space states will consist of link-partons derived from the Fourier expansion of  $M$ . For sufficiently large  $a$ ,  $M$  remains a massive degree of freedom and there is an energy barrier for the addition of a link-parton to a Fock state. Operators of order  $M^p$  in  $P^-$  will connect Fock states differing by at most  $p - 2$  link-partons. By expanding  $P^-$  to a given order of  $M$  in this regime (the colour-dielectric expansion) we therefore cut off interactions between lower-energy few-parton states and higher-energy many-parton states. Note that all energy scales are still allowed however, since we take the  $\mathcal{L} \rightarrow \infty$  limit, enabling highly virtual small  $p^+$  partons to appear. The advantage of a cut-off on changes of parton number is that it organises states into a constituent hierarchy, consistent with energetics.

The Lagrangian density satisfying condition (A) can be written

$$L_{\mathbf{x}} = \bar{D}_{\alpha} M_r(\mathbf{x})(\bar{D}^{\alpha} M_r(\mathbf{x}))^{\dagger} - V_{\mathbf{x}} - U_{\mathbf{x}} \quad (5)$$

where the ‘potential’ has a purely transverse part  $V_{\mathbf{x}}$  and a mixed part  $U_{\mathbf{x}}$ . Up to 4th order in  $M$ , the purely transverse part is

$$\begin{aligned} V_{\mathbf{x}} = & -\frac{\beta}{Na^2} \text{Tr} \left\{ M_1(\mathbf{x}) M_2(\mathbf{x} + a\hat{1}) M_1^{\dagger}(\mathbf{x} + a\hat{2}) M_2^{\dagger}(\mathbf{x}) \right\} + \text{c.c.} \\ & + \sum_r \mu^2 \text{Tr} \{ M_r M_r^{\dagger} \} + \sum_r \frac{\lambda_0}{a^2 N} (\det[M_r] + \det[M_r^{\dagger}]) \\ & + \sum_r \frac{\lambda_1}{a^2 N} \text{Tr} \{ M_r M_r^{\dagger} M_r M_r^{\dagger} \} + \frac{\lambda_2}{a^2 N} \sum_r \text{Tr} \{ M_r(\mathbf{x}) M_r(\mathbf{x} + a\hat{r}) M_r^{\dagger}(\mathbf{x} + a\hat{r}) M_r^{\dagger}(\mathbf{x}) \} \\ & + \sum_r \frac{\lambda_3}{a^2 N^2} (\text{Tr} \{ M_r M_r^{\dagger} \})^2 + \frac{\lambda_4}{a^2 N} \sum_{\sigma=\pm 2, \sigma'=\pm 1} \text{Tr} \{ M_{\sigma}^{\dagger} M_{\sigma} M_{\sigma'}^{\dagger} M_{\sigma'} \} \\ & + \frac{4\lambda_5}{a^2 N^2} \text{Tr} \{ M_1 M_1^{\dagger} \} \text{Tr} \{ M_2 M_2^{\dagger} \} . \end{aligned} \quad (6)$$

---

<sup>2</sup>This assumption is not warranted in the presence of finite-mass fermions. The subtlety lies in  $p^+ = 0$  vacuum modes that are not recovered even as  $\mathcal{L} \rightarrow \infty$ . For Yukawa interactions of finite-mass fermions, parity certainly isn’t recovered in the naïve way [23].

The  $\det[M]$  term can be dropped if  $N > 4$  and can always be neglected in the large- $N$  limit. The mixed part, to the approximation we will need, can be written

$$U_{\mathbf{x}} = \sum_{\mathbf{y}} \epsilon_{\alpha\beta} \text{Tr} \{ E_{\mathbf{x}} P_{\mathbf{xy}} F^{\alpha\beta}(\mathbf{y}) P_{\mathbf{xy}}^\dagger \} - G^2 f(E_{\mathbf{x}}) , \quad (7)$$

where  $E_{\mathbf{x}}$  is a non-dynamical pseudoscalar adjoint field at site  $\mathbf{x}$ , while  $P_{\mathbf{xy}}$  is a linear combination of Wilson lines in  $M$ , each from  $\mathbf{x}$  to  $\mathbf{y}$  (for gauge invariance). Upon integrating out  $E$ , the function  $f(E) = \text{Tr}\{E^2\} + O(E^4)$  gives a simple  $\frac{1}{2G^2} \text{Tr}\{F^{\alpha\beta} F_{\alpha\beta}\}$  term if only the  $E^2$  part is retained and we set  $P_{\mathbf{xy}} = \delta_{\mathbf{xy}}$ .<sup>3</sup> This will be the only term needed for pure gauge theory to  $O(M^4)$  once  $A_\alpha$  has been eliminated. We gave the more general form in Eqn. (7) since it will be relevant in the heavy-source analysis.

From the above Lagrangian, four of the usual seven kinematic Poincaré generators derived canonically from the energy-momentum tensor  $T^{\mu\nu}$  remain gauge invariant and can be made kinematic by LF gauge choice  $A_- = 0$ . They are, at  $x^+ = 0$  say,

$$P^+ = 2 \int dx^- \sum_{\mathbf{x},s} \text{Tr} \{ \partial_- M_s(\mathbf{x}) \partial_- M_s(\mathbf{x})^\dagger \} , \quad (8)$$

$$M^{+-} = 2 \int dx^- \sum_{\mathbf{x},s} x^- \text{Tr} \{ \partial_- M_s(\mathbf{x}) \partial_- M_s(\mathbf{x})^\dagger \} \quad (9)$$

$$M^{+r} = -2 \int dx^- \sum_{\mathbf{x},s} \left( x^r + \frac{a}{2} \delta^{rs} \right) \text{Tr} \{ \partial_- M_s(\mathbf{x}) \partial_- M_s(\mathbf{x})^\dagger \} \quad (10)$$

We will use these to define states of definite momentum  $\{P^+, \mathbf{P}\}$ . The other three would-be kinematic Poincaré generators in light-front formalism,  $\{P^r, M^{12}\}$ , are not gauge-invariant when derived canonically from  $T^{\mu\nu}$  because of the lattice cut-off; the simplest gauge-invariant extensions are no longer quadratic in fields, even in LF gauge.

Of the dynamic generators, the most important, and the only one we explicitly treat, is the light-front Hamiltonian itself

$$P^- = \int dx^- \sum_{\mathbf{x}} \left( V_{\mathbf{x}} - \text{Tr} \{ A_+(\mathbf{x}) J^+(\mathbf{x}) \} - \frac{1}{G^2} \text{Tr} \{ \partial_- A_+ \partial_- A_+ \} \right) , \quad (11)$$

$$J^+(\mathbf{x}) = i \sum_r \left( M_r(\mathbf{x}) \overleftrightarrow{\partial}_- M_r^\dagger(\mathbf{x}) + M_r^\dagger(\mathbf{x} - a\hat{r}) \overleftrightarrow{\partial}_- M_r(\mathbf{x} - a\hat{r}) \right) . \quad (12)$$

Rather than trying to directly construct an approximate realisation of the Poincaré algebra at finite cut-off, we will minimise cut-off artifacts by optimising restoration of Lorentz covariance in low-energy eigenstates of the Hamiltonian  $P^-$ .

In the light-front gauge,  $A_+$  is a non-dynamical variable and eliminating it introduces non-local interactions thus

$$P^- = \int dx^- \sum_{\mathbf{x}} \left( \frac{G^2}{4} \text{Tr} \left\{ \frac{J^+ J^+}{\partial_- \partial_-} \right\} - \frac{G^2}{4N} \text{Tr} \left\{ \frac{J^+}{\partial_-} \right\} \text{Tr} \left\{ \frac{J^+}{\partial_-} \right\} + V_{\mathbf{x}} \right) \quad (13)$$

where  $J^+/\partial_- \equiv \partial_-^{-1}(J^+)$ . There is still a residual  $x^-$ -independent gauge invariance generated by the charge  $\int dx^- J^+$ . As originally shown in Refs. [6, 7], finite energy states  $|\Psi\rangle$  are subject to

<sup>3</sup>The case  $P_{\mathbf{xy}} = \delta_{\mathbf{xy}}$  is related to the generalised 2DQCD of M. Douglas *et al.* [26]

the gauge singlet condition  $\int dx^- J^+ |\Psi\rangle = 0$ . In the large- $N$  limit, this means that Fock space at fixed  $x^+$  is formed by connected closed loops of link variables  $M$  on the transverse lattice (the  $x^-$  co-ordinate of each  $M$  is unrestricted).

## 2.2 Quantisation

The dynamical problem is now to diagonalise  $P^-$  at fixed total momenta  $\{P^+, \mathbf{P}\}$ . A convenient basis consists of free link-partons obtained from the Fourier modes  $a(k^+, \mathbf{x})$  of  $M$  in the  $x^-$  co-ordinate

$$M_r(x^+ = 0, x^-, \mathbf{x}) = \frac{1}{\sqrt{4\pi}} \int_0^\infty \frac{dk^+}{\sqrt{k^+}} \left( a_{-r}(k^+, \mathbf{x}) e^{-ik^+ x^-} + a_r^\dagger(k^+, \mathbf{x}) e^{ik^+ x^-} \right). \quad (14)$$

The Fock space formed from creation operators  $a^\dagger$  in the large- $N$  limit, and other details of the calculation in this Fock space, including construction of states of definite momentum, have been described elsewhere [9, 10]. We applied both DLCQ and Tamm-Dancoff cut-offs in Fock space, extrapolating both of these at fixed values of the couplings in Eqn. (6).<sup>4</sup>

Low-energy eigenfunctions of  $P^-$  (*id est* glueballs) are to be tested for Lorentz covariance, the couplings appearing in Eqn. (6) being tuned to minimise covariance violations. Since  $G^2N$ , with dimension (energy)<sup>2</sup>, is consistent with 't Hooft's large- $N$  limit [27], we will use it to set the dimensionful scale. Thus, the dispersion relation of a glueball can be written

$$2P^+P^- = G^2N \left( \mathcal{M}_0^2 + \mathcal{M}_1^2 a^2 |\mathbf{P}|^2 + 2\overline{\mathcal{M}}_1^2 a^2 P^1 P^2 + O(a^4 |\mathbf{P}|^4) \right). \quad (15)$$

For each glueball,  $\mathcal{M}_i^2$  are dimensionless functions of the couplings which, for a given set of couplings, are extracted by expanding eigenvalues of  $P^-$  in  $a\mathbf{P}$ . A truly relativistic state must have an isotropic speed of light

$$\begin{aligned} a^2 G^2 N \mathcal{M}_1^2 &\equiv c_{\text{on}}^2 = 1 \\ a^2 G^2 N (\mathcal{M}_1^2 + \overline{\mathcal{M}}_1^2) &\equiv c_{\text{off}}^2 = 1. \end{aligned} \quad (16)$$

$c_{\text{on}}$  is the speed of light in direction  $\mathbf{x} = (1, 0)$ ;  $c_{\text{off}}$  is the speed of light in the direction  $\mathbf{x} = (1, 1)$ . In addition, the an-harmonic corrections at  $O(a^4 |\mathbf{P}|^4)$  must vanish, but we will not use this condition directly.

The ratio of transverse to longitudinal scales is set by the dimensionless combination  $a^2 G^2 N$ . This can be deduced from two measurements of the string tension  $\sigma$ , for example [28]. The first measures the mass squared of winding modes on a periodic transverse lattice, fitting the groundstate to  $n^2 a^2 \sigma_T^2$  for winding number  $n$ . The second measures the heavy-source potential in the continuous  $x^3$  direction, fitting the groundstate to  $\sigma_L R$  for separation  $R$ .<sup>5</sup> Demanding  $\sigma_T = \sigma_L \equiv \sigma$  and expressing eigenvalues in units of  $G^2N$ , we may eliminate  $\sigma$  and deduce  $a^2 G^2 N$ . We may also deduce  $G^2N$ , and hence all dimensionful quantities, in units of  $\sigma$ . Some refinements we have made to the calculation of the heavy-source potential, since our previous work, are described in the next subsection.

<sup>4</sup>The largest cut-offs used were a  $K = 26/2$  DLCQ resolution and 8-link Tamm-Dancoff cut-off in the glueball sector, while a  $K = 70/2$  and 4-link cut-off was used in the heavy-source sector. The latter sector has an additional cut-off  $P_{\text{max}}^+$ , as discussed in Ref. [10], which was varied up to 7.

<sup>5</sup>One could also use the heavy-source potential in transverse directions to find  $\sigma_T$ , but it is more accurate to use winding modes for this.



### 2.3 Heavy-source potential $V_{QQ}$

The non-relativistic heavy-source potential  $V_{QQ}$  provides us with a number of important pieces of information. The string tension  $\sigma$  will be used as our basic physical unit for dimensionful quantities. The deviations of the potential from rotational invariance will help to fix couplings in the theory. We find that, in general, both relativistic invariance in the glueball sector and rotational invariance in the heavy-source sector are needed to accurately pin down the effective LF Hamiltonian.

The heavy-source sector was first studied on the transverse lattice in 2+1 dimensions by Burkardt and Klindworth [28]. They used the most rudimentary approximation to the Lagrangian, quadratic in the link and heavy-source fields. Along both the continuous and lattice spatial directions linear potentials arise, which can be given the same slope  $\sigma$  by adjusting the link-field mass  $\mu^2$  for given  $a/\sqrt{\sigma}$ . The authors of Ref. [28] observed that the contours of the potential in the spatial plane were ‘square’ at  $\mu^2 = \infty$  ( $a \sim \infty$ ) and ‘circular’ at  $\mu^2 = 0$  ( $a \sim 1/\sqrt{\sigma}$ ). This rounding of the potential indicates that rotational invariance is improved as the lattice spacing is reduced, as one would hope. However, there is still a potentially large violation of rotational invariance due to the fact that any discrepancy between the tensions measured in continuum and lattice directions can be masked by adjusting  $a$ . Only by examining another sector where the lattice spacing value is used, such as covariance of glueballs, can one tell whether the potential is truly circular or merely oval. Using more accurate higher order LF Hamiltonians in the pure glue sector [10, 17], we found that the values of the lattice spacing deduced from rotational invariance of the heavy-source potential were not very compatible with those needed for relativistic covariance of glueballs. Therefore one needs to also improve the accuracy in the heavy-source sector. We take some steps in this direction in the following.

Our light-front treatment of heavy-source fields  $\phi_i$ , which we take to be scalars in the fundamental representation, has been introduced in Ref. [10]. We will work with a LF Hamiltonian in LF gauge  $A_- = 0$  to order  $M^4$  in the pure glue operators, order  $M^2$  in the heavy-source operators, leading order of the heavy-source mass  $\rho$ , together with the conditions discussed in Section 2. This LF Hamiltonian for heavy sources with non-zero spatial separation can be derived from the Lagrangian density

$$L_{\mathbf{x}} = \sum_r \text{Tr} \left\{ \bar{D}_\alpha M_r(\mathbf{x}) \left( \bar{D}^\alpha M_r(\mathbf{x}) \right)^\dagger \right\} - \frac{1}{2G^2} \text{Tr} \{ F^{\alpha\beta} F_{\alpha\beta} \} - V_{\mathbf{x}} + (D_\alpha \phi)^\dagger D^\alpha \phi - \rho^2 \phi^\dagger \phi - \frac{\tau_1}{NG^2} \text{Tr} \{ F^{\alpha\beta} F_{\alpha\beta} W_r \} - \frac{\tau_2}{NG^2} \text{Tr} \{ M_r^\dagger(\mathbf{x}) F^{\alpha\beta}(\mathbf{x}) M_r(\mathbf{x}) F_{\alpha\beta}(\mathbf{x} + a\hat{r}) \} , \quad (17)$$

where

$$W_r = (M_r^\dagger M_r + M_r M_r^\dagger) . \quad (18)$$

In addition, there are combinations which are suppressed in the  $\rho \rightarrow \infty$  limit, such as  $\phi^\dagger W_r \phi$ ,  $\phi^\dagger F^{\alpha\beta} F_{\alpha\beta} \phi$ , which we did not include in this work.<sup>6</sup>

After gauge fixing  $A_- = 0$ , eliminating  $A_+$  in powers of  $M$ , and discarding the higher orders in  $M$ , the LF Hamiltonian resulting from (17) is

$$P^- = \int dx^- \sum_{\mathbf{x}, r} \frac{G^2}{4} \text{Tr} \left\{ \frac{J_{\text{tot}}^+}{\partial_-} \frac{J_{\text{tot}}^+}{\partial_-} \right\} - \frac{G^2}{4N} \text{Tr} \left\{ \frac{J_{\text{tot}}^+}{\partial_-} \right\} \text{Tr} \left\{ \frac{J_{\text{tot}}^+}{\partial_-} \right\} + V_{\mathbf{x}}$$

<sup>6</sup>We investigated the first of these terms in earlier work by scaling its coefficient with  $\rho$  so that it survived the  $\rho \rightarrow \infty$  limit. It had little affect on the string tension but seemed to help short-distance rotational invariance.

$$+\rho^2\phi^\dagger\phi + \frac{2\tau_1}{N} \text{Tr} \left\{ \frac{J^+}{\partial_-} \frac{J^+}{\partial_-} W_r \right\} + \frac{2\tau_2}{N} \text{Tr} \left\{ \frac{J^+(\mathbf{x})}{\partial_-} M_r(\mathbf{x}) \frac{J^+(\mathbf{x} + a\hat{r})}{\partial_-} M_r^\dagger(\mathbf{x}) \right\} \quad (19)$$

with

$$J_{\text{tot}}^+ = J^+ + i\phi \overleftrightarrow{\partial}_- \phi^\dagger \quad (20)$$

The diagonalisation of this Hamiltonian in Fock space proceeds in a similar way to the glueball sector (see Ref. [10]).

The selection (17) is more general than was used in previous calculations. Physically speaking, the new terms  $\tau_1$  and  $\tau_2$  generate oscillations of the flux string perpendicular to  $x^3$ -separated sources (via enhanced pair production of links) as required of a rough gauge string [29]. This partially screens the linear potential in the  $x^3$ -direction to produce a rotationally invariant  $\sigma$ . However, while we find that these new terms improve the interaction between heavy sources at zero and one-link transverse separation, small- $x^3$  separations and wider transverse separations are left unimproved. This will result in a loss of off-axis rotational invariance, which could only be remedied by including terms at  $O(M^4)$  *et cetera*. The underlying difficulty in getting rotational invariance may be related to the existence of a roughening transition separating the large  $a$  regime from the continuum in the heavy-source sector.

### 3 Space of Hamiltonians

Our procedure for extracting Lorentz-covariant cut-off independent results is non-standard, so we take some time in this section to describe the procedure we used for the present calculation.

#### 3.1 Topology

Abstractly, we have a set of cut-off Hamiltonians containing in principle an infinite number of operators  $O_i$  with couplings  $g_i$ . For simplicity, we consider only one high-energy cut-off  $1/a$ , all others having been removed by extrapolation.<sup>7</sup>  $\mathcal{H}$  is the infinite-dimensional space of the  $g_i$ , the space of Hamiltonians.

One could in  $\mathcal{H}$  define renormalisation group trajectories as trajectories along which, say, the eigenvalues of the Hamiltonian are invariant. We are particularly interested in a trajectory on which Lorentz covariance is restored — the ‘Lorentz trajectory’  $\mathcal{T}$  — for observables containing no explicit momenta above the cut-off. Perry and Wilson [30] have emphasised the idea, albeit in weak-coupling perturbation theory, that when a symmetry is restored in a cut-off theory, the number of couplings running independently with the cut-off is reduced. For Lorentz symmetry in pure gauge theory, for example, this coherent running of the couplings should pick out  $\mathcal{T} \subset \mathcal{H}$ . A basic hypothesis of our approach to pure  $SU(N)$  gauge theory on the transverse lattice will be that a single one-parameter Lorentz trajectory extends from the continuum to quite low cut-offs. In order to test the hypothesis, we will specify conditions for an approximate Lorentz trajectory  $\mathcal{T}_s$  in a finite-dimensional subspace  $\mathcal{H}_s \subset \mathcal{H}$ . The subspace  $\mathcal{H}_s$  arises from the conditions we placed on the Hamiltonian in Section 2. The most straightforward way to define  $\mathcal{T}_s$  is in terms of a finite selection of observables contributing to a  $\chi^2$  test for deviations from Lorentz covariance. At the same time,

<sup>7</sup>This extrapolation in itself may require tuning of the  $g_i$  in general. However, such tuning is not necessary for pure gauge theories within the approximations we make.

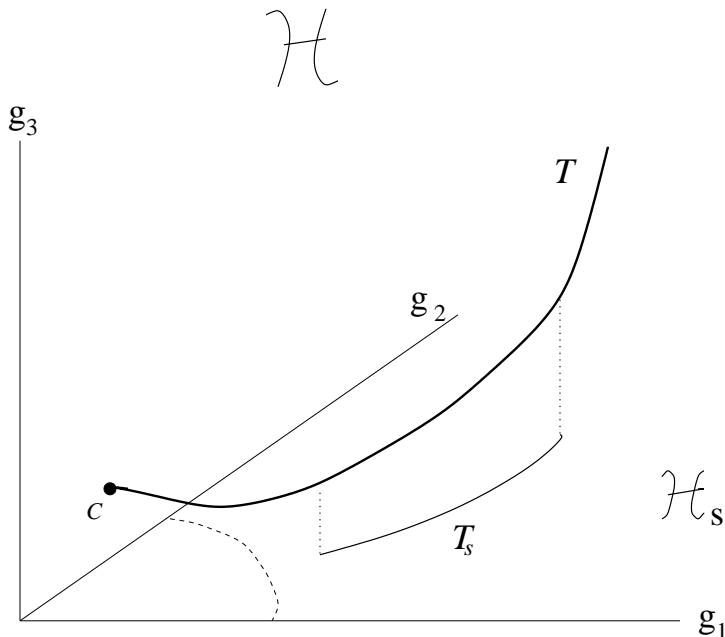


Figure 2: The space  $\mathcal{H} = \{g_1, g_2, g_3, \dots\}$  of Hamiltonians and its subspace  $\mathcal{H}_s = \{g_1, g_2\}$ .  $\mathcal{T}$  is the exact Lorentz trajectory,  $\mathcal{T}_s$  the approximation to it in  $\mathcal{H}_s$ .  $\mathcal{C}$  is the intersection of  $\mathcal{T}$  with the continuum  $1/a = \infty$ . The dashed line is a possible phase boundary in  $\mathcal{H}_s$  separating  $\mathcal{T}_s$  from the continuum.

we believe that it should be possible to develop tests of Lorentz covariance that do not depend on a specific choice of observables, *exempli gratia* ensuring closure of the Poincaré algebra. But we have yet to carry out this development.

Figure 2 illustrates the space of Hamiltonians we have in mind. The space  $\mathcal{H} = \{g_1, g_2, g_3, \dots\}$  represents the infinite-dimensional space of couplings. The cut-off  $1/a$  decreases along the Lorentz trajectory  $\mathcal{T}$  as one moves away from the intersection of  $\mathcal{T}$  with the continuum,  $\mathcal{C}$ . A finite-dimensional subspace  $\mathcal{H}_s$  is denoted by the  $g_3 = 0$  plane.  $\mathcal{T}$  will not lie entirely in  $\mathcal{H}_s$  in general, so the best one can do is investigate approximations in  $\mathcal{H}_s$ . We search  $\mathcal{H}_s$  over a certain range of cutoffs for a trajectory  $\mathcal{T}_s$  which minimises the distance to  $\mathcal{T}$ , *id est* minimises violations of Lorentz covariance. It is not sufficient to simply find an isolated point in  $\mathcal{H}_s$  at which violations of Lorentz covariance are minimised. This may have little to do with  $\mathcal{T}$ . One must establish an entire trajectory. If  $\mathcal{T}$  does not exist for the range of cut-off investigated, or lies far from  $\mathcal{H}_s$ , one will be unable to find an unambiguous trajectory  $\mathcal{T}_s$ , and the method fails.

The metric to determine the distance from  $\mathcal{T}$  is the  $\chi^2$  test for Lorentz covariance, which involves both a choice of observables and their relative weights. Even if  $\mathcal{T}$  exists, a random choice of  $\chi^2$  observables and their weights will make it difficult to identify. Consistent with the colour-dielectric expansion, we gave higher weights to low energy observables dominated by a few link-partons and made sure that the number of observables was always  $\gg \dim[\mathcal{H}_s]$ .

Having convinced oneself that  $\mathcal{T}_s$  is uniquely established for the metric employed and the range of cut-off investigated, one can use it to estimate the value of observables on  $\mathcal{T}$ . Observables will exhibit approximate scaling along  $\mathcal{T}_s$ , by virtue of its nearness to  $\mathcal{T}$  (which is an exact scaling

trajectory). The values of these observables will be close to the values on  $\mathcal{T}$ , and the violations of scaling *and* covariance as one moves along  $\mathcal{T}_s$  can be used to estimate the systematic error from use of a finite-dimensional space of Hamiltonians. As one enlarges the space  $\mathcal{H}_s$ , *exempli gratia* by going to higher orders of the colour-dielectric expansion, one can get closer to  $\mathcal{T}$  and the errors reduce.

This procedure is to be contrasted with the traditional perturbative ‘improvement’ program of introducing irrelevant operators in a cut-off theory. There, one derives the couplings via perturbative renormalisation group transformations, solves the theory, and extrapolates to the continuum. This is the approach to LF Hamiltonians being pursued by a number of authors [12]. Instead, we use symmetry directly to construct coupling trajectories, making the assumption that symmetry uniquely fixes the values of observables in QCD, once the overall scale has been specified. In practice, we do not construct renormalisation group trajectories and do not extrapolate to the continuum.

We do not try to extrapolate the results to  $a = 0$  because in  $\mathcal{H}_s$  there may be barriers to the continuum (*exempli gratia* roughening or large- $N$  transitions). Our use of disordered massive link variables  $M$ , together with the concomitant expansion of  $P^-$  in powers of  $M$ , means that the transverse lattice spacing  $a$  is quite coarse in the region of  $\mathcal{H}$  we search. However, by definition, there can be no phase boundaries separating  $\mathcal{T} \subset \mathcal{H}$  from the continuum. Provided a suitable  $\mathcal{T}$  exists, and we can get close enough to it, the interpolation of phase boundaries only breaks the connection between scaling violations in each phase of  $\mathcal{H}_s$ , not the estimate of the observable itself.

### 3.2 Topography

We now construct a set of topographical charts of  $\mathcal{H}_s$  that help one to decide whether a unique Lorentz trajectory exists. It is convenient to use  $G^2N$  to set the dimensionful scale wherever possible, and introduce dimensionless versions of the other couplings as the co-ordinates of  $\mathcal{H}_s$

$$m^2 = \frac{\mu^2}{G^2N}, \quad l_i = \frac{\lambda_i}{a^2G^2N}, \quad t_i = \frac{\tau_i}{\sqrt{G^2N}}, \quad b = \frac{\beta}{a^2G^2N}. \quad (21)$$

We employed two ways to search  $\mathcal{H}_s$ .

**Method 1** For a given  $m^2$ , this minimises  $\chi^2$  over all couplings  $\{l_1, l_2, l_3, l_4, l_5, b\}$  to give a one-parameter trajectory in  $\mathcal{H}_s$ . This amounts to a direct determination of  $\mathcal{T}_s$ .

**Method 2** For a given  $m$  and  $g_i \in \{l_1, l_2, l_3, l_4, l_5, b\}$ , this minimises  $\chi^2$  over all the remaining couplings. There is a chart for each  $g_i$  which can be displayed as a contour plot with heights  $\chi_{min}^2$ . The existence of  $\mathcal{T}$  should show up as a unique valley on each chart, universal with respect to small changes in the form of the metric, the bottom of the valley coinciding with the trajectory  $\mathcal{T}_s$  found by Method 1.

With Method 1, in a reasonable amount of time we could extrapolate the DLCQ and Tamm-Dancoff cut-offs before using a routine to iteratively search for the minimum value of  $\chi^2$ , setting the mass scale from first principles via string tension measurements. Because of its more time-consuming nature, a number of compromises were necessary to obtain decent results by Method 2: the DLCQ and Tamm-Dancoff cut-offs were fixed;<sup>8</sup> to avoid the extra complication introduced by the heavy-source analysis, the mass scale was fixed by setting  $\mathcal{M}(0^{++}) = 3.5\sqrt{\sigma}$ , a result which had been deduced from

---

<sup>8</sup> $K = 6/2$  and a 6-link truncation.

$m$	$l_1$	$l_2$	$l_3$	$l_4$	$l_5$	$b$	$t_1$	$t_2$	$\chi^2$
0.0444	0.012	-0.068	437	0.097	182	0.429	-0.795	-0.702	13.36
0.0890	-0.005	-0.075	426	0.118	197	0.504	-0.908	-0.864	14.28
0.1342	-0.035	-0.079	463	0.132	211	0.575	-0.999	-1.008	15.99
0.1803	-0.038	-0.090	374	0.158	143	0.688	-1.086	-1.094	18.76
0.2275	-0.037	-0.101	62.4	0.212	18.8	0.858	-1.205	-1.189	21.14
0.2765	-0.048	-0.137	111	0.208	22.4	0.962	-1.147	-1.185	25.28
0.3275	-0.007	-0.144	60.7	0.163	9.6	1.010	-0.788	-0.734	31.87
0.3812	-0.007	-0.195	12.3	0.308	2.28	1.381	-1.207	-1.302	31.83
0.4384	-0.047	-0.175	50	0.331	12.5	1.530	0.588	-0.635	43.35
0.500	0.319	-0.313	822	0.367	318	1.906	-1.42	-1.605	59.78

Table 1: The trajectory which minimises the  $\chi^2$  test of Lorentz covariance.

Method 1 on  $\mathcal{T}_s$  (see later); we used fixed values  $l_3 = 100$  and  $l_5 = 10$ , again motivated by the typical values on  $\mathcal{T}_s$  from Method 1. The very large couplings  $l_3$  and  $l_5$  have a special significance which is explained in Ref. [10]. They can be set to virtually any very large value for a Lorentz-covariant theory.

The first step in the process requires some experimentation with different  $\chi^2$  variables. In general, we used the isotropy of glueball dispersion relations, rotational invariance of the heavy-source potential, and Lorentz multiplet structure of the low-lying glueball spectrum as the ingredients in  $\chi^2$ . After some fine-tuning of weights, we found a very clear signal for a trajectory  $\mathcal{T}_s$  running from small to large  $m$  on which the  $\chi^2$  was significantly reduced to about one per effective degree of freedom. Fig. 3 and Table 1 show the trajectory found by Method 1. Further details of the  $\chi^2$  choice are available in a data file [31]. 40 variables were used in  $\chi^2$ , though 15 of these were given significantly more weight than the others, corresponding to groundstate observables in each symmetry sector. The lowest values of  $\chi^2$ , in the range 10–20, occur on a smooth trajectory through the lowest four non-zero values of  $m$  sampled, above which  $\mathcal{T}_s$  begins to break up somewhat. Fig. 4 shows the global topography of coupling space via Method 2, confirming that the trajectory found in Method 1 sits at the bottom of a well-defined, unique valley. (Note that regions giving tachyonic glueballs were assigned  $\chi^2 = \infty$  for the purposes of Fig. 4).

Physically one expects  $m^2 \rightarrow -\infty$  as  $a \rightarrow 0$ , since  $M$  should be forced to lie on the  $SU(N)$  group manifold  $M^\dagger M = 1$  in the continuum limit. Since we have limited ourselves to the region  $m^2 > 0$ , we are some way from the continuum. It is remarkable, therefore, that such a strong signal for the Lorentz trajectory  $\mathcal{T}$  is obtained. We can deduce the lattice spacing in units of  $\sigma$  on  $\mathcal{T}_s$  if we assume no scaling violations; see Fig. 5. Naïvely one expects  $m$  to increase with  $a$ , but measurements of  $a$  vs.  $m$  are very sensitive to scaling violations. Fig. 5 is roughly consistent for the smallest  $m$  region, though scaling violations appear much stronger in  $3 + 1$  dimensions than they were in  $2 + 1$ -dimensions [10].

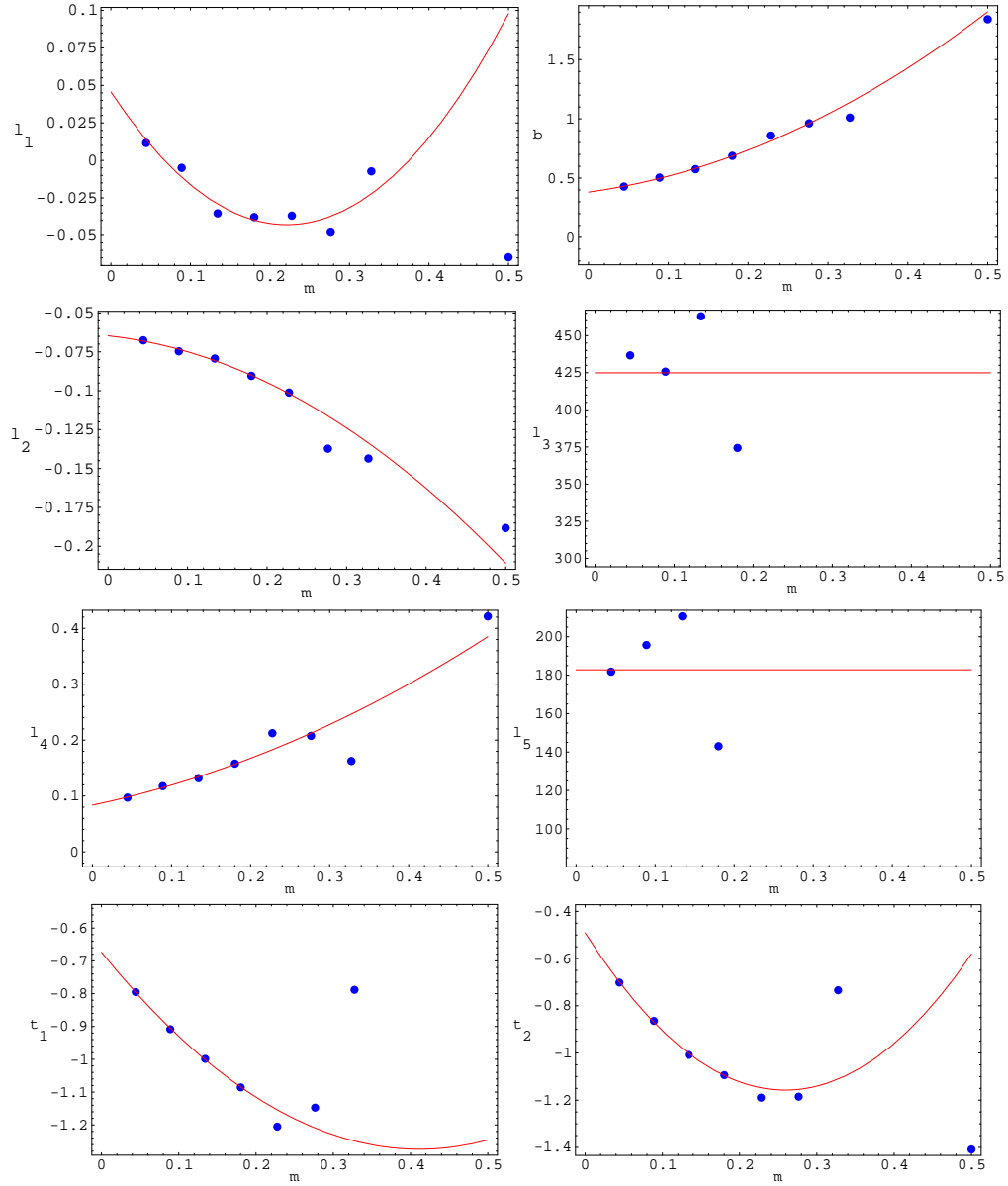


Figure 3: The couplings along  $\mathcal{T}_s$ .

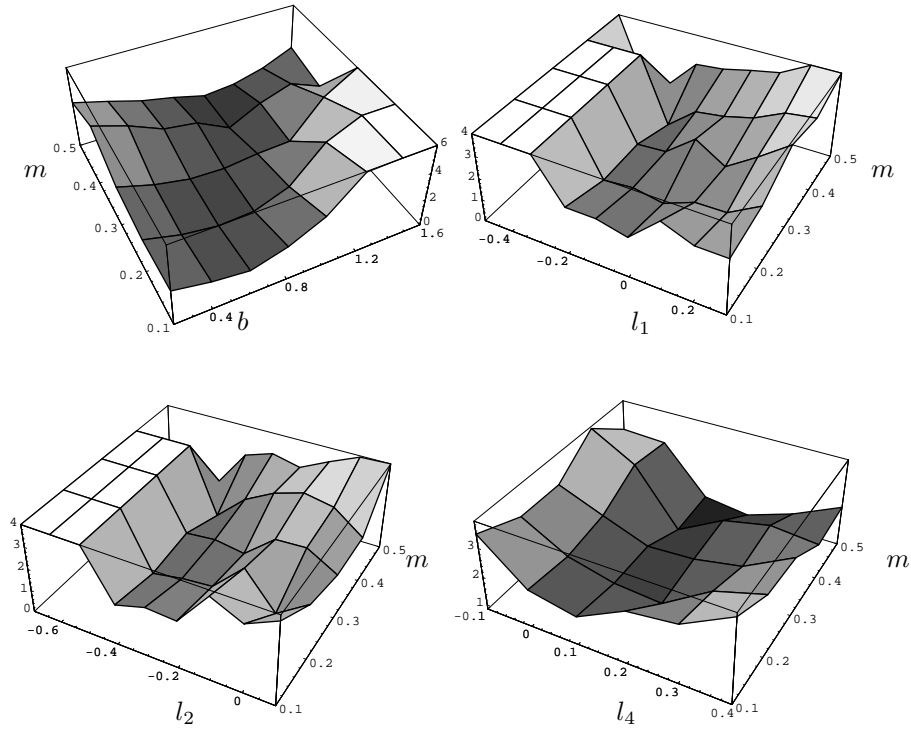


Figure 4: Charts of coupling space with  $\chi_{\min}^2$  as the height variable.

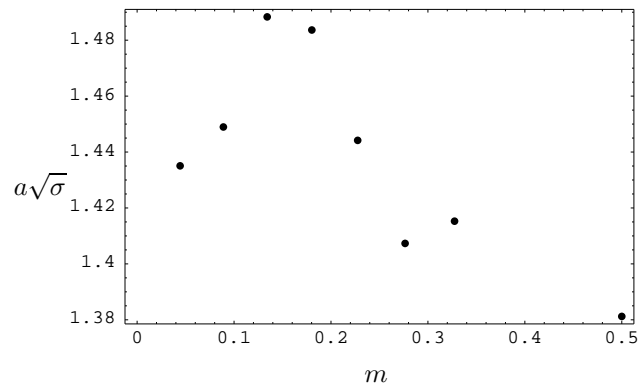


Figure 5: The variation of the lattice spacing  $a$  with link-field mass  $m$  along  $\mathcal{T}_s$ , assuming exact scaling holds (this only holds, even approximately, at small  $m$ ).

$\mathcal{J}^{\mathcal{PC}}$	$ \mathcal{J}_3 ^{\mathcal{P}_1}$	$c_{\text{on}}$	$c_{\text{off}}$	$\frac{\mathcal{M}}{\sqrt{\sigma}}$
$0^{++}$	$0^+$	1.07	1.07	3.50(24)
$2^{++}$	$2^+$	0.86	0.87	4.97(68)
	$2^-$	Im	–	6.07(?)
	$1^\pm$	0.91, Im	0.72, Im	5.62(?)
	$0^+$	0.99	0.98	4.97(18)
$1^{+-}$	$1^\pm$	0.88, 1.06	0.94, 1.00	5.37(36)
	$0^-$	1.07	1.07	5.74(45)

Table 2: The glueball multiplet components at the lowest overall  $\chi^2 = \chi_o^2$ , showing masses from  $\mathcal{M}^2 = 2P^+P^-(\mathbf{P} = 0)$  and  $c$  from the dispersion relation (15). “Im” indicates  $c^2 < 0$  and “–” indicates the quantity has not been measured. The  $\mathcal{J}_3 = \pm 1$  states are exactly degenerate.

## 4 Glueball data

### 4.1 Masses

In the limit  $\mathcal{L} \rightarrow \infty$ , in addition to  $x^3$ -boost invariance, the transverse lattice has exact discrete symmetries of the group  $D_4$  [7], together with charge-conjugation  $\mathcal{C}$ . Reflections  $\mathcal{P}_1$  and  $\mathcal{P}_2$ , about  $x_1 = 0$  and  $x_2 = 0$  respectively, can be used to estimate parity  $\mathcal{P} = \mathcal{P}_1\mathcal{P}_2\mathcal{P}_3$  from free-field estimates of the light-front parity  $\mathcal{P}_3 : x^+ \leftrightarrow x^-$ . 90-degree rotations  $x^1 \rightarrow x^2$  are exact and can be used to distinguish the angular momentum projections  $\mathcal{J}_3 = 0, \pm 1, \pm 2$  from each other.

In Fig. 6, we plot the scaling behaviour of the lightest glueball masses  $\mathcal{M}$  along  $\mathcal{T}_s$ , labelled by  $|\mathcal{J}_3|^{\mathcal{P}_1}$  and grouped into would-be Spin–Parity–Charge–Conjugation multiplets  $\mathcal{J}^{\mathcal{PC}}$ . We have estimated error bars on each datum by combining well-understood (and small) DLCQ and Tamm-Dancoff extrapolation errors ( $\sim 0.03\mathcal{M}$ ) with an estimate of systematic finite- $a$  errors coming from violations of Lorentz covariance, using the formula

$$\mathcal{M}(\chi_o^2) \frac{\chi^2}{\chi_o^2} |c - 1|_{\text{av.}} . \quad (22)$$

$|c - 1|_{\text{av.}}$  is the averaged deviation of the speed of light in transverse directions  $\mathbf{x}$ , relative to direction  $x^3$ . The datum of lowest overall  $\chi^2 = \chi_o^2$  occurs at  $m = 0.044$ . Formula (22), which is supposed to represent roughly the uncertainty of the intercept  $\mathcal{M}$  of the dispersion relation, works well for nearly covariant glueballs in  $2 + 1$ -dimensional studies where the ‘exact’ mass is known [11, 10]. It is also consistent with the magnitude of scaling violations and Lorentz multiplet splittings in the present case. The various components of a Lorentz multiplet in Fig. 6 become rapidly more covariant, measured by their isotropy and degeneracy, as  $m$  is reduced.<sup>9</sup>

The final mass estimates given in the introduction are displayed in more detail in Table 2. They are taken from the point of lowest  $\chi^2 = \chi_o^2 = 13.36$  on the scaling trajectory. We are confident that

<sup>9</sup> Naïvely, one might expect the colour-dielectric expansion to break down at the very smallest  $m$ , as the link fields become very light. However, the energy barrier to production of more links comes principally from gauge self-energy contributions at these small masses [7, 24, 32].



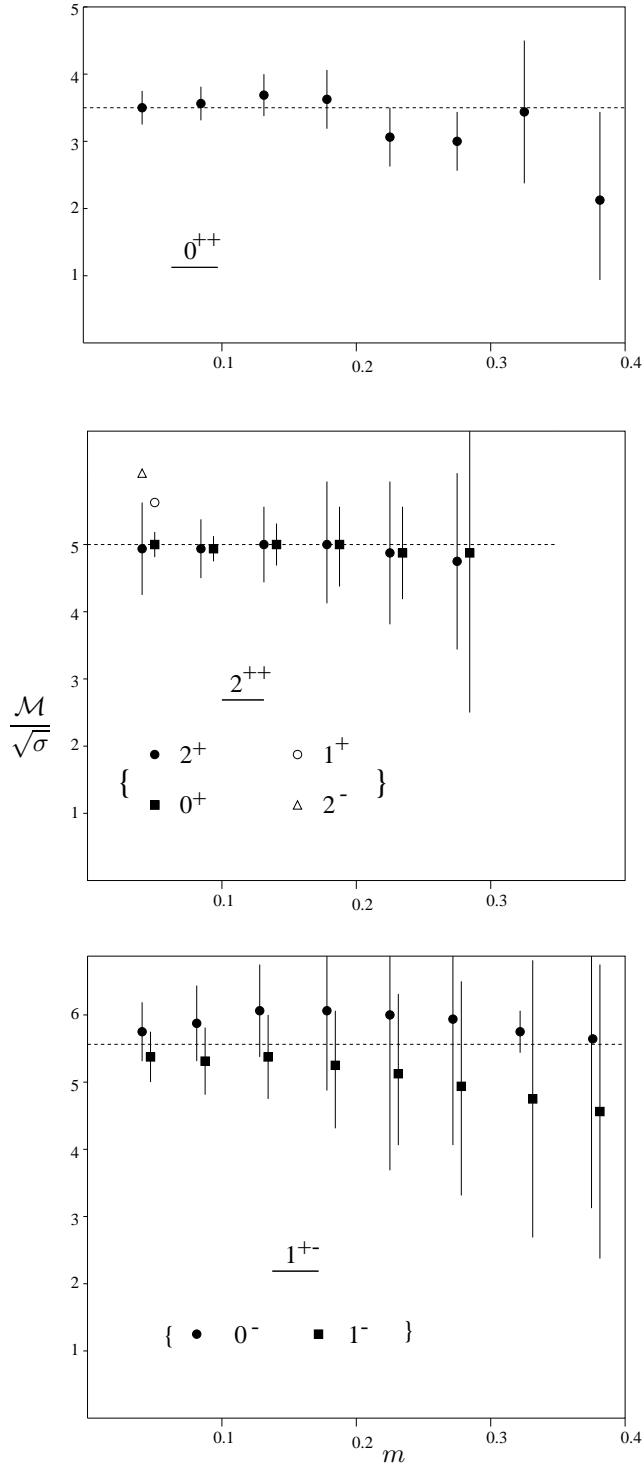


Figure 6: The variation of glueball masses with link-field mass  $m$  along  $\mathcal{T}_s$ . The open-symbol data for the  $2^{++}$ , which are plotted only at  $\chi^2 = \chi_o^2$ , are still too inaccurate for error estimates. Data at given  $m$  are displaced horizontally for clarity.

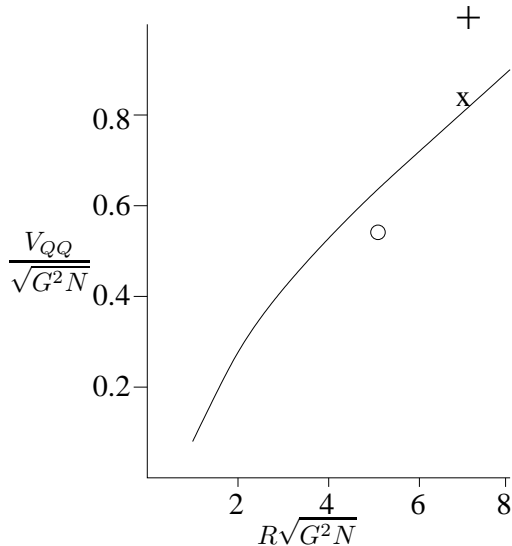


Figure 7: Heavy-source potential  $V_{QQ}$  vs. source separation  $R = \sqrt{(\delta x^3)^2 + (\delta x^2)^2 + (\delta x^1)^2}$ . Shown is a fit to the measured potential at zero transverse separations  $\delta x^1 = \delta x^2 = 0$ . The ‘off-axis’ data are: (O)  $\delta x^3 = 1.22$ ,  $\delta x^2 = 4.95$ ,  $\delta x^1 = 0$ ; (X)  $\delta x^3 = 4.89$ ,  $\delta x^2 = 4.95$ ,  $\delta x^1 = 0$ ; (+)  $\delta x^3 = 0$ ,  $\delta x^2 = 4.95$ ,  $\delta x^1 = 4.95$ . Units are  $(G^2N)^{-1/2}$ .

the value of and error on these results is a reasonable estimate of the continuum result, provided the relevant observable exhibits a scaling region along  $\mathcal{T}_s$  and the error (22) is small. We emphasise that scaling alone is not sufficient for a good estimate of the continuum result. Table 2 gives some idea of where the remaining errors lie. In particular, the  $\mathcal{P}_1 = -1$  components of the tensor glueball are still dominated by lattice artifacts, requiring further terms in the Hamiltonian presumably. Our lightest  $0^{-+}$  state lies at  $\sim 8\sqrt{\sigma}$ , compared to much lower  $SU(3)$  Euclidean lattice Monte Carlo results [20]; but we have no measure of its covariance and suspect a very large error on our result.

It is interesting to plot glueball masses in pure gauge theory versus  $1/N^2$ , since this is supposed to be the relevant expansion parameter about  $N = \infty$  [27]; see Fig. 1 in the introduction. There is remarkably little variation of glueball masses with the number of colours. It gives further support to the notion that  $N = 3$  is close to  $N = \infty$  in many situations. In particular, popular flux-tube [33] and string models [34] of the soft gluonic structure of hadrons are typically more appropriate to the large- $N$  limit of QCD (or are independent of  $N$ ). Figure 1 indicates that these models should give worthwhile quantitative approximations to  $N = 3$  pure QCD. One can even go so far as to derive a formula for glueball masses at any  $N$ , by fitting those at  $N = 2, 3, \dots, \infty$  to polynomials in  $1/N^2$ ; this might be a useful guide for higher- $N$  ELMC studies [35].

## 4.2 Covariance

In searching for  $\mathcal{T}_s$  we used data from the heavy-source potential and glueball dispersion near  $\mathbf{P} = 0$  (the speed of light). At the  $\chi^2 = \chi_0^2$  point on  $\mathcal{T}_s$ , the potential is plotted in Fig. 7. The potential between sources separated by distance  $R$  only in the  $x^3$  direction has been fit to

$$\frac{V_{QQ}}{\sqrt{G^2N}} = 0.084R\sqrt{G^2N} + 0.259 - \frac{0.265}{R\sqrt{G^2N}}. \quad (23)$$

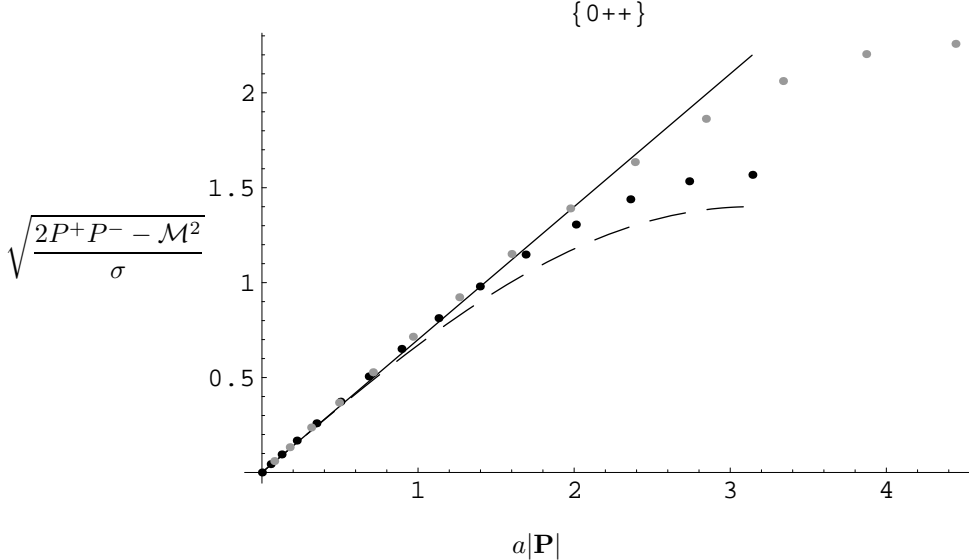


Figure 8: Dispersion relation of  $0^{++}$  glueball. Straight line is exact relativistic form, dots are data at  $\chi^2 = \chi_0^2$  point on  $\mathcal{T}_s$  (black for direction  $\mathbf{P} \propto (1,0)$ , gray for  $\mathbf{P} \propto (1,1)$ ). The dashed line is a ‘lattice’ dispersion  $\propto \sqrt{1 - \cos a|\mathbf{P}|}$  along  $\mathbf{P} \propto (1,0)$ , normalised to the correct slope at  $\mathbf{P} = 0$ .

The remaining points in Fig. 7 are ‘off- $x^3$ -axis’ samples of the potential at a general separation  $R$ , whose deviations from the value given by (23) are used in the  $\chi^2$  test. As can be seen, the rotational invariance of the potential is patchy, showing significant deviations at very small  $x^3$  separations and/or along the  $(1,1)$  transverse direction (see discussion in Section 2.3).

Only the long range form of the glueball dispersion was used as a variable in the  $\chi^2$  test. As a further consistency check, we can also plot the dispersion throughout the Brillouin zone  $0 < |\mathbf{P}| < \pi/a$ . As the example of the lightest  $0^{++}$  glueball illustrates (Fig. 8), improvement towards the full relativistic form seems to occur on  $\mathcal{T}_s$ .

### 4.3 Wavefunctions

From the explicit glueball eigenfunctions one can extract various measurements of glueball structure.<sup>10</sup> While these results are still somewhat academic until one couples quarks to allow the glueballs to decay, they are still important. One can check whether the constituent structure of boundstates is valid. The probability distribution of transverse shapes is a useful measure of this (see Table 3). If eigenfunctions were to contain large mixtures of different numbers of link-partons, it would call into question the validity of the colour-dielectric expansion.

Another interesting quantity is the distribution of longitudinal momentum  $P^+$  among the link

<sup>10</sup>The results in this subsection are from an earlier calculation that used a slightly different choice of  $\chi^2$  test than that appropriate to Table 1. The difference in the resulting wavefunctions is negligible for the purposes of our discussion in this subsection.

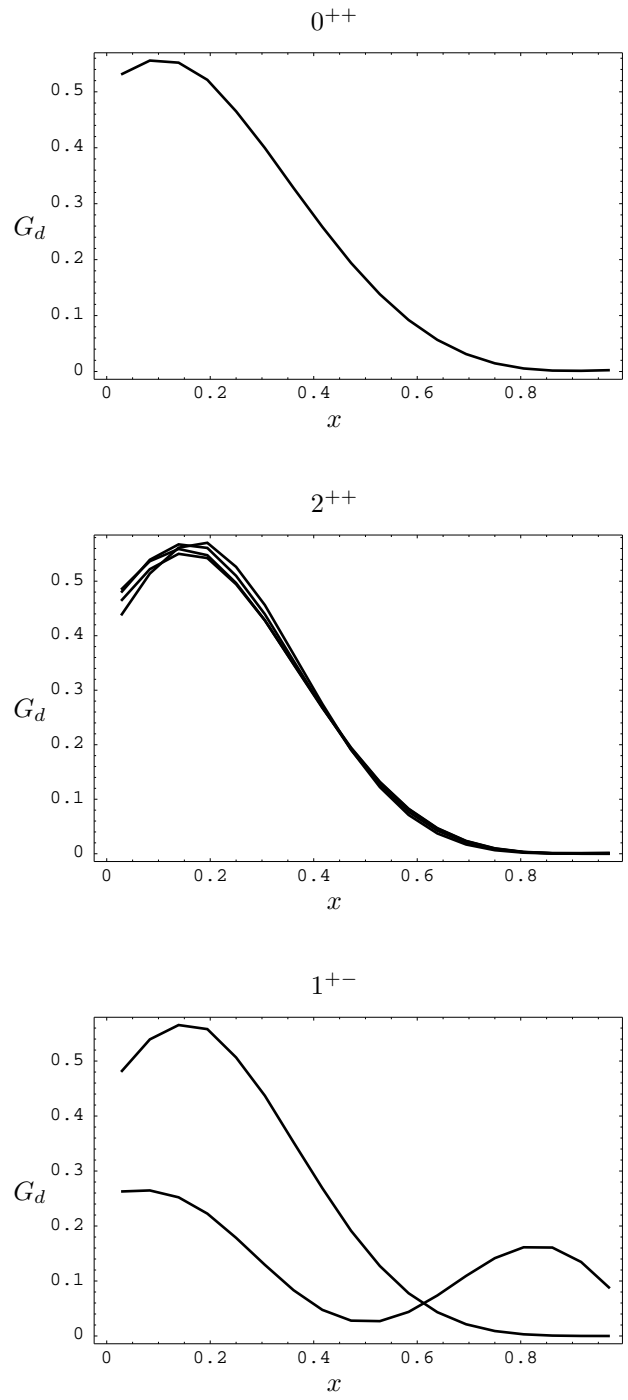


Figure 9: The distribution of  $P^+$  momentum in various  $J_3$  components of the low-lying glueballs.

Shape	scalar		tensor			vector	
	{0 <sup>+</sup> }	{2 <sup>+</sup> }	2 <sup>-</sup>	1 <sup>±</sup>	0 <sup>+</sup> }	{1 <sup>±</sup> }	0 <sup>-</sup> }
$m$	0.019	0.016	0	0	0.014	0.810	0
$l_2$	0.003	0.518	0	0	0.535	0.039	0
$l_1$	0.002	0.369	0	0	0.361	0.016	0
$l_4$	0.483	0	0.882	0.923	0.017	0.052	0.049
$b$	0.400	0	0.024	0	0.003	0.069	0.860
other	0.093	0.097	0.094	0.077	0.070	0.014	0.091

Table 3: Probability distribution of transverse shapes for various  $|\mathcal{J}_3|^{P_1}$  components of the low-lying glueball eigenfunctions (following Table 2). The shapes are denoted by the coupling constant for that shape in  $P^-$ ; for example,  $m$  denotes the  $\text{Tr}\{M_r M_r^\dagger\}$  operator. Contributions  $< 0.001$  are neglected.

partons. In Fig. 9 we plot the quantity

$$G_d(x, 1/a) = \frac{1}{2\pi x P^+} \int dx^- e^{-ix P^+ x^-} \langle \Psi(P^+) | \text{Tr}\{\partial_- M_r \partial_- M_r^\dagger\} | \Psi(P^+) \rangle, \quad (24)$$

which measures (in  $A_- = 0$  gauge) the probability of finding a link-parton carrying momentum fraction  $x$  of the glueball momentum  $P^+$ . It depends upon the transverse normalisation scale through  $a$ , though our piece of the Lorentz trajectory is too short to reliably see physical evolution of  $G_d$  with scale.  $a \sim 0.65$  fm for the data shown.

$G_d$  is related to the gluon distribution; it becomes the gluon distribution in the limit  $a \rightarrow 0$ . Moreover, since  $M$  is some collective gluon excitation and the momentum sum rule is satisfied, one would naïvely expect the gluon distribution at a general scale  $a$  to be softer than  $G_d$ . In this case, the  $0^{++}$  glueball (Fig. 9) does not resemble gluonium (two-gluon boundstate), which would have a distribution symmetric about  $x = 0.5$ . The fact that all components of the tensor's distribution look like the  $0^{++}$  is also interesting. It may indicate that the tensor's angular momentum comes mostly from gluon spin; however we caution that not all components of our tensor are yet behaving in a covariant fashion. Once light quarks are coupled to the problem, these distributions should have distinctive experimental signatures.

## 5 Conclusions

In this paper we have carried through the program, first suggested by Bardeen *et al.* [7], for solving the boundstate problem of pure QCD on a transverse lattice. Three of our developments were crucial to this success: inclusion of higher Fock sectors via DLCQ; inclusion of the full set of allowed operators occurring to lowest order of the colour-dielectric expansion of the light-front Hamiltonian; efficient semi-analytic methods for computing and extrapolating many-body light-front Hamiltonians [9, 10]. In addition, we combined the analysis of the pure glue sector with an analysis of the heavy source sector, which is needed not only to provide an absolute scale but also to pin down the correct

Lorentz-covariant Hamiltonian in each sector. The upshot of all these developments is that we were able to clearly identify a scaling trajectory in the space of couplings on which Lorentz covariance of observables is enhanced.

We believe that this trajectory is an approximation to the exact Lorentz-covariant, scaling trajectory in the infinite dimensional space of all Hamiltonians. Strong evidence in favour of this comes from the scaling behaviour of glueball masses, whose values agree with continuum results (extrapolated to large- $N$ ) from established methods. It is largely straightforward to relax the approximations we made so far, including the large- $N$  limit, to increase the scope and accuracy of our results.

The light-front wavefunctions are entirely new results. Their accuracy is largely undetermined and, in their present form, they cannot easily be used to compute an experimentally measured quantity. However, their interesting structure might provide a source for phenomenological models. In fact, given the accuracy of the glueball masses and covariance of the dispersion relations, we would be very surprised to find that they were inaccurate.

To make contact between light-front wavefunctions and the wealth of hadronic experimental data, the next step must introduce finite-mass propagating quarks. Although overviews of the standard Kogut-Susskind [6] and Wilson [36] fermions on a transverse lattice have been given, no first-principles calculations in the manner of this paper have been completed. By adding observables that test chiral symmetry (and parity) we can hope to find a similar scaling trajectory. Such calculations are now underway.

Acknowledgements: We thank our colleagues in DAMTP, CERN, Erlangen and the ILCAC and especially M. Teper for help and encouragement at various stages. SD is supported by PPARC grant No. GR/LO3965.

## References

- [1] P. A. M. Dirac, *Rev. Mod. Phys.* **21** (1949) 392.
- [2] S. J. Brodsky, H.-C. Pauli, and S. Pinsky, *Phys. Rep.* **301** (1998) 299.
- [3] G. P. Lepage and S. J. Brodsky, *Phys. Rev.* **D22** (1980) 2157; in *Perturbative Quantum Chromodynamics*, A. H. Mueller, ed. (World Scientific, Singapore 1989).
- [4] H.-C. Pauli and S. J. Brodsky, *Phys. Rev.* **D32** (1985) 1993 and 2001.
- [5] K. G. Wilson *et al.*, *Phys. Rev.* **D49** (1994) 6720.
- [6] W. A. Bardeen and R. B. Pearson, *Phys. Rev.* **D14** (1976) 547.
- [7] W. A. Bardeen, R. B. Pearson, and E. Rabinovici, *Phys. Rev.* **D21** (1980) 1037.
- [8] S. Dalley and B. van de Sande, *Nucl. Phys.* **B53** (Proc. Suppl.) (1997) 827.
- [9] S. Dalley and B. van de Sande, *Phys. Rev.* **D56** (1997) 7917.
- [10] S. Dalley and B. van de Sande, *Phys. Rev.* **D59** (1999) 065008.
- [11] M. Teper, *Phys. Rev.* **D59** (1999) 014512.
- [12] S. D. Glazek and K. G. Wilson, *Phys. Rev.* **D47** (1993) 4657; *Phys. Rev.* **D48** (1993) 5963; *Phys. Rev.* **D49** (1994) 4214;  
R. J. Perry, Lectures at *Hadrons 94*, Gramado, Brasil (1994) hep-th/9407056;  
M. M. Brisudova and R. J. Perry, *Phys. Rev.* **D54** (1996) 1831 and 6453;  
M. M. Brisudova, R. J. Perry, and K. G. Wilson, *Phys. Rev. Lett.* **78** (1997) 1227;  
M. M. Brisudova, S. Szpigiel, and R. J. Perry, *Phys. Lett.* **B421** (1998) 334;  
B. H. Allen and R. J. Perry, *Phys. Rev.* **D58** (1998) 125017; hep-th/990812;  
R. D. Kylin, B. H. Allen, and R. J. Perry, *Phys. Rev.* **D60** (1999) 067704;  
S. D. Glazek, *Phys. Rev.* **D57** (1998) 3558; *Acta Phys. Polon.* **B29** (1998) 1979; hep-th/9904029;  
T. S. Walhout, *Phys. Rev.* **D59** (1999) 065009.
- [13] K. G. Wilson, *Phys. Rev.* **D10** (1974) 2445.
- [14] J. B. Kogut and L. Susskind, *Phys. Rev.* **D11** (1975) 395.
- [15] P. A. Griffin, *Nucl. Phys.* **B139** (1992) 270.
- [16] S. Dalley and I. R. Klebanov, *Phys. Lett.* **B298** (1993) 79; *Phys. Rev.* **D47** (1993) 2517;  
K. Demeterfi, I. R. Klebanov, and G. Bhanot, *Nucl. Phys.* **B418** (1994) 15.
- [17] S. Dalley and B. van de Sande, *Phys. Rev. Lett.* **82** (1999) 1088.
- [18] G. Bali *et al.* (UKQCD-Wuppertal), *Phys. Lett.* **B309** (1993) 378;  
J. Sexton *et al.*, *Phys. Rev. Lett.* **75** (1995) 4563.
- [19] C. Michael and M. Teper, *Phys. Lett.* **B199** (1987) 95; *Nucl. Phys.* **B305** (1988) 453; *Nucl. Phys.* **B314** (1989) 327.

- [20] C. Morningstar and M. Peardon, Phys. Rev. **D56** (1997) 4043; Phys. Rev. **D60** (1999) 0345509.
- [21] S. Samuel, Phys. Rev. **D55** (1997) 4189;  
 X.Q. Luo and Q.Z. Chen, Mod. Phys. Lett. **A11** (1996) 2435;  
 E. Gubankova, C-R. Ji, and S. R. Cotanch, hep-ph/9908331 and hep-ph/9905527;  
 B. H. Allen and R. J. Perry, E-print in Ref. [12].
- [22] C. Csaki, H. Ooguri, Y. Oz, and J. Terning, JHEP 9901 (1999) 017;  
 R. de Mello Koch, A. Jevicki, M. Mihailescu, and J. P. Nunes, Phys. Rev. **D58** (1998) 105009;  
 C. Csaki, Y. Oz, J. Russo, and J. Terning, Phys. Rev. **D59** (1999) 065012.
- [23] A. Harindranath and R. J. Perry, Phys. Rev. **D43** (1991) 4051;  
 M. Burkardt and A. Langnau, Phys. Rev. **D44** (1991) 1187 and 3857;  
 M. Burkardt, Phys. Rev. **D54** (1996) 2913.
- [24] F. Antonuccio and S. Dalley, Nucl. Phys. **B461** (1996) 275.
- [25] B. van de Sande and M. Burkardt, Phys. Rev. **D53** (1996) 4628.
- [26] M. R. Douglas, K. Li, and M. Staudacher, Nucl. Phys. **B420** (1994) 118.
- [27] G. 't Hooft, Nucl. Phys. **B72** (1974) 461; Nucl. Phys. **B75** (1974) 461.
- [28] M. Burkardt and B. Klindworth, Phys. Rev. **D55** (1997) 1001; in *Confinement III*, Newport News VA (1998), hep-ph/9809283.
- [29] C. Itzykson, M. E. Peskin, and J-B. Zuber, Phys. Lett. **B95** (1980) 259;  
 A. Hasenfratz, E. Hasenfratz, and P. Hasenfratz, Nucl. Phys. **B180** (1981) 353;  
 M. Luscher, G. Munster, and P. Weisz, Nucl. Phys. **B180** (1981) 1;  
 M. Luscher, Nucl. Phys. **B180** (1981) 317.
- [30] R. J. Perry and K. G. Wilson, Nucl. Phys. **B403** (1993) 587.
- [31] Data files are available on the Internet at: <http://www.geneva.edu/~bvds>.
- [32] F. Antonuccio and S. Dalley, Phys. Lett. **B376** (1996) 154.
- [33] H. B. Nielsen and P. Olesen, Nucl. Phys. **B57** (1973) 367;  
 N. Isgur and J. Paton, Phys. Rev. **D31** (1985) 2910.
- [34] Y. Nambu, Proc. Int. Conf. on Symm. and Quark Model, Wayne State Univ. 1969, Gordon and Breach, London 1970; Phys. Rev. **D10** (1974) 4262;  
 L. Susskind, Phys. Rev. **D1** (1970) 1182.
- [35] M. J. Teper, Phys. Lett. **B397** (1997) 223.
- [36] M. Burkardt and H. El-Khozondar, Phys. Rev. **D60** (1999) 054504.